



Minerva Access is the Institutional Repository of The University of Melbourne

**Author/s:**

Chen, X;Cui, J;Ping, Y;Suma, T;Cavalieri, F;Besford, QA;Chen, G;Braunger, JA;Caruso, F

**Title:**

Probing cell internalisation mechanics with polymer capsules

**Date:**

2016-10-21

**Citation:**

Chen, X., Cui, J., Ping, Y., Suma, T., Cavalieri, F., Besford, Q. A., Chen, G., Braunger, J. A. & Caruso, F. (2016). Probing cell internalisation mechanics with polymer capsules. *Nanoscale*, 8 (39), pp.17096-17101. <https://doi.org/10.1039/c6nr06657g>.

**Persistent Link:**

<https://hdl.handle.net/11343/120177>

## Probing Cell Internalisation Mechanics with Polymer Capsules

Xi Chen,<sup>a</sup> Jiwei Cui,<sup>a</sup> Yuan Ping,<sup>a</sup> Tomoya Suma,<sup>a</sup> Francesca Cavalieri,<sup>a</sup> Quinn A. Besford,<sup>a</sup> George Chen,<sup>b</sup> Julia A. Braunger,<sup>a</sup> and Frank Caruso<sup>a\*</sup>

Received 00th January 20xx,  
Accepted 00th January 20xx

DOI: 10.1039/x0xx00000x

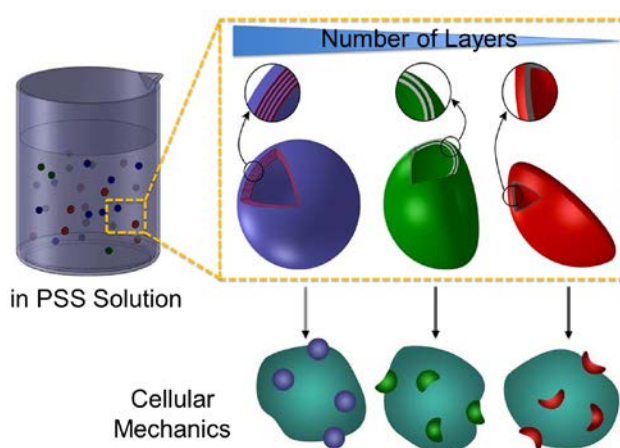
www.rsc.org/

**We report polymer capsule-based probes for quantifying the pressure exerted by cells during capsule internalisation ( $P_{in}$ ). Poly(methacrylic acid) (PMA) capsules with tuneable mechanical properties were fabricated through layer-by-layer assembly. The  $P_{in}$  was quantified by correlating the cell-induced deformation with the ex situ osmotically induced deformation of the polymer capsules. Ultimately, we found that human monocyte-derived macrophage THP-1 cells exerted up to approximately 360 kPa on the capsules during internalisation.**

Elucidating the interactions between nanomaterials and biological systems (nano-bio interactions) is important for advancing understanding in the fields of cell biology, tissue engineering, and nanomedicine.<sup>1-5</sup> Nano- and microparticles have received interest as promising therapeutic delivery carriers and as sensors due to their tuneable and unique physicochemical properties.<sup>6,7</sup> In this regard, most studies have investigated the physicochemical properties of particles, for example size, shape, and surface chemistry, with the aim of modulating their cellular interactions.<sup>8,9</sup> The mechanical properties of the particles, such as stiffness, influence how the particles interact with biological cells, and also how the cells can alter the properties of particles. For example, recent studies have reported the deformation of polymer nano- or microparticles upon association with cells.<sup>10-13</sup> The deformation of polymer particles caused by cells can influence the fate of the polymer particles and the payload release profile inside the capsules. The deformation of polymer particles is cell line dependent, highlighting the importance of tailoring their mechanical properties for a diverse panel of cell lines. It is therefore of interest to investigate the ability of cells

to deform polymer particles during the internalisation process.

Polymer particles have the potential to act as probes to reveal information about cellular processes.<sup>14,15</sup> For example, our previous study reported the formation of layer-by-layer (LbL) assembled polymer capsules with in-built endocytic pH-coupled fluorescent switches that display reversible “on/off” fluorescence in response to cellular pH changes. This made it possible to monitor cellular internalisation in live cells, as the pH varies from approximately neutral outside a cell (pH 7.4) to acidic environments in the endosomes and lysosomes (pH 4.7-6.3).<sup>16</sup> Recently, Liu et al. reported nanosensors, employing polymer particles cross-linked via disulfide bonds, for the detection of intracellular glutathione (GSH) during cellular uptake.<sup>17</sup> By varying the cross-linking density of disulfide bonds, a series of nanosensors that are sensitive to intracellular GSH concentration were fabricated. The above studies demonstrate that carefully tailoring the physicochemical properties of the polymer particles may



**Scheme 1** LbL-assembled polymer capsules with a different number of polymer layers as capsule probes for assessment of internalisation pressure,  $P_{in}$ , of live cells.  $P_{in}$  is obtained by correlating the ex situ osmotic pressure applied by a PSS ( $M_w$  1MDa) solution to capsule deformation.

<sup>a</sup>ARC Centre of Excellence in Convergent Bio-Nano Science and Technology, and the Department of Chemical and Biomolecular Engineering, The University of Melbourne, Parkville, Victoria 3010, Australia. E-mail: fcaruso@unimelb.edu.au

<sup>b</sup>Department of Chemical and Biomolecular Engineering, The University of Melbourne, Parkville, Victoria 3010, Australia.

\*Present address: School of Materials Science and Engineering, Nanyang Technological University, Singapore 639798, Singapore.

†Electronic Supplementary Information (ESI) available: Experimental methods, additional figures, and tables. See DOI: 10.1039/x0xx00000x

reveal greater information on cellular processes.

The mechanical properties of polymer particles have been studied using both anisotropic or isotropic forces.<sup>10,12,18</sup> Delcea et al. studied the deformation characteristics of polymer microcapsules upon cellular internalisation using atomic force microscopy (AFM).<sup>12</sup> The combined analysis of the degree of deformation of the polymer capsules by an ex situ AFM experiment, and an in situ cellular internalisation experiment, allowed the mechanical forces during the cellular uptake process to be estimated. From the ex situ experiment, it was estimated that Vero cells exerted a force of at least 0.2  $\mu\text{N}$  upon intracellular incorporation of the microcapsules. However, to mimic intracellular mechanical forces, isotropic compression provides a more realistic model compared with an anisotropic local force as applied to polymer capsules by AFM tips.<sup>19</sup> Gao et al. reported that thin-shelled polymer capsules are osmotically and isotropically deformed in poly(styrene sulfonate) (PSS,  $M_w$  70 kDa) solution.<sup>18</sup> Because the capsule wall is permeable to small molecules but impermeable to the high molecular weight polymers and associated counterions, the difference of polymer concentration between the interior and exterior of capsules generates osmotic pressure that causes the capsules to deform. This method can therefore be used to determine the mechanical strength of polymers capsules subjected to either isotropic osmotic pressure or mechanical stress.<sup>20</sup> Additionally, the method allows studies on a large number of capsules simultaneously, which is in contrast to AFM.<sup>21</sup>

Herein, we report polymer capsule-based probes for quantifying the pressure exerted by cells during capsule internalisation. Poly(methacrylic acid) (PMA) capsules with tuneable mechanical properties were fabricated through LbL assembly. By increasing the number of polymer layers in the capsule shell, a range of PMA capsules with different shell thickness, and consequently different mechanical stiffness,

was produced. Deformation of the polymer capsules was evaluated from osmotic pressure-induced deformation in bulk PSS solutions of varying concentration. Subsequently, the intracellular deformation of the PMA capsules was investigated in human monocyte-derived macrophage THP-1 cells (dTHP-1). Capsule deformation in the intracellular milieu was verified by direct visualisation using super-resolution structured illumination microscopy (SIM). The pressure exerted on the capsules during cellular internalisation ( $P_{in}$ ) was quantified by evaluating the extent of deformation of the capsules with different mechanical stiffness (Scheme 1). We found that the dTHP-1 cells exert an internalisation pressure of up to 357 kPa  $\pm$  13 kPa on the submicron-sized polymer capsules.

PMA capsules composed of a different number of polymer layers, ranging from three to ten, were prepared through the LbL assembly technique according to our previous studies.<sup>22</sup> Briefly,  $\text{SiO}_2$ -particle templates of 0.52  $\mu\text{m}$ -diameter were alternately coated with thiolated PMA and poly(N-vinylpyrrolidone) (PVPON), followed by cross-linking the thiol groups on PMA into thioether bonds (Fig. S1, ESI<sup>†</sup>). PMA capsules were obtained after dissolution of the  $\text{SiO}_2$  templates and removal of the sacrificial PVPON layers. Alexa Fluor 633 (AF633)-labelled PMA capsules were imaged in cell culture medium by SIM (Fig. S2, ESI<sup>†</sup>). The diameter of the polymer capsules (0.7  $\mu\text{m}$ ) was negligibly affected by the number of deposited layers (Table S1, ESI<sup>†</sup>). The film thickness of the PMA capsule shells, determined by AFM height analysis (Fig. 1A–H), proportionally increased with the number of polymer layers (Fig. S3 and Table S2, ESI<sup>†</sup>).

The osmotically induced deformation of PMA capsules was investigated in bulk PSS solutions. PSS with a molecular weight of 1 MDa was chosen due to the impermeability of high molecular weight polymers to PMA capsules. In previous work, the permeability of PMA capsules with four layers and a low

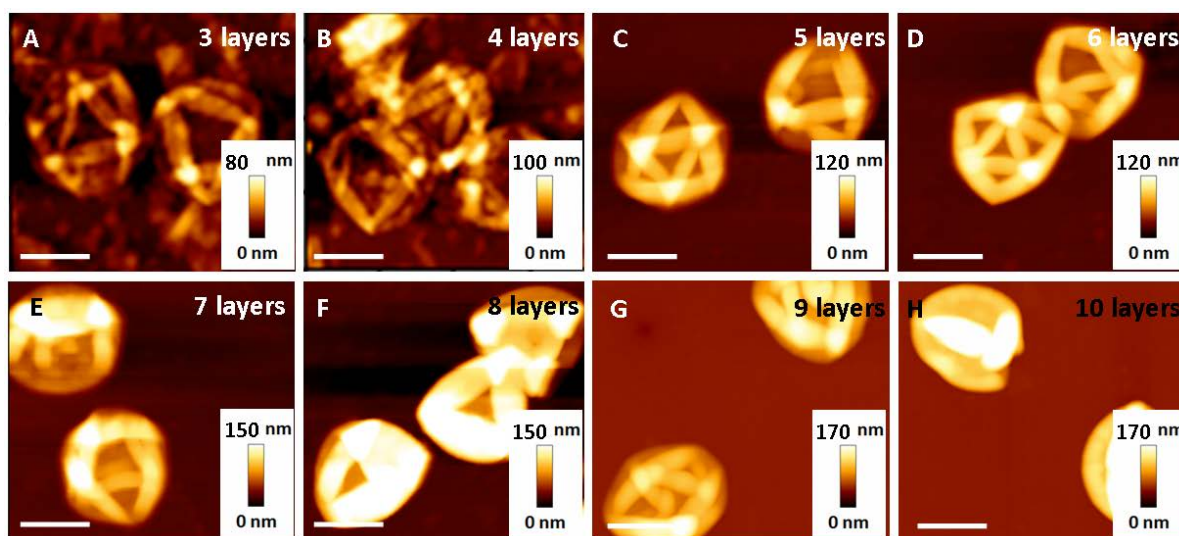


**Fig. 1** AFM images of PMA capsules composed of a different number of polymer layers: three (A), four (B), five (C), six (D), seven (E), eight (F), nine (G), and 10 layers (H). Scale bars are 1  $\mu\text{m}$ . Note that the capsules are air-dried for AFM, resulting in a crumpled appearance.

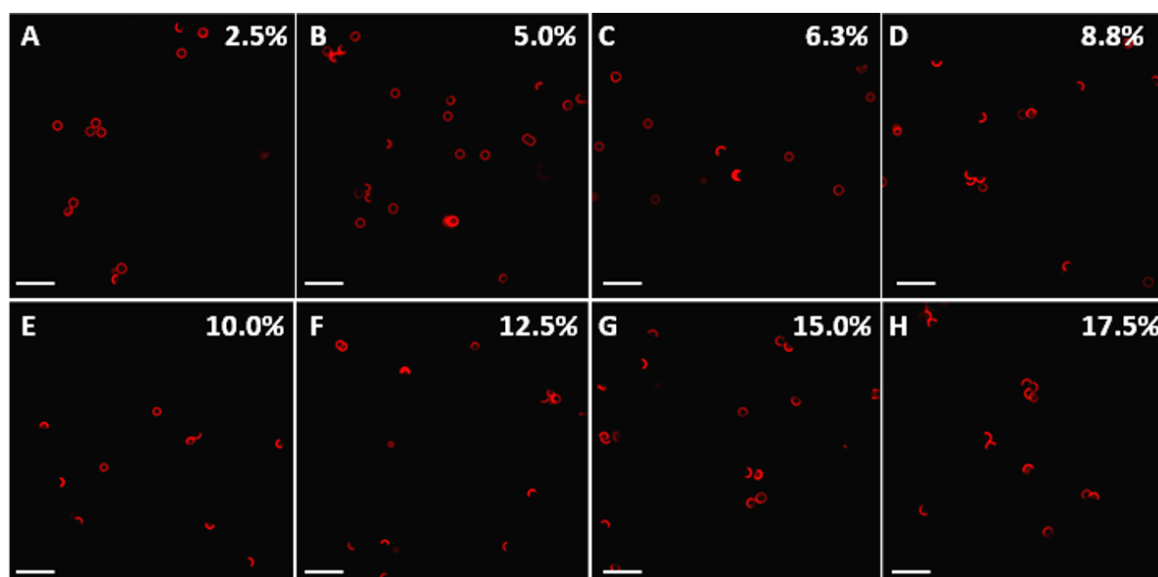


**Fig. 2** Osmotic pressure-induced deformation of PMA capsules consisting of six polymer layers by PSS ( $M_w$  1 MDa) solutions at different concentrations: 2.5 (A), 5.0 (B), 6.3 (C), 8.8 (D), 10.0 (E), 12.5 (F), 15.0 (G), and 17.5 wt% (H). SIM images are presented at the maximum intensity projection and the scale bars are 2.5  $\mu\text{m}$ .

degree of cross-linking was shown to be impermeable to encapsulated 15 kDa PMA, therefore consolidating our choice of 1 MDa PSS for this study.<sup>23</sup> PMA capsules were mixed in PSS solutions of varying concentration, from 2.5% to 17.5%, for 2 h, followed by SIM imaging.

Our results show that the capsules exhibit different degrees of deformation as a function of PSS concentration.

Taking PMA capsules with six polymer layers as an example, most capsules did not deform at a low PSS concentration (2.5–6.3 wt%, Fig. 2A–C), indicating that the generated osmotic pressure was not high enough to overcome the elastic restoring force of the capsule shells.<sup>10</sup> In contrast, at higher PSS concentrations (8.8–17.5 wt%, Fig. 2D–H), most capsules were deformed into a crescent-like shape.

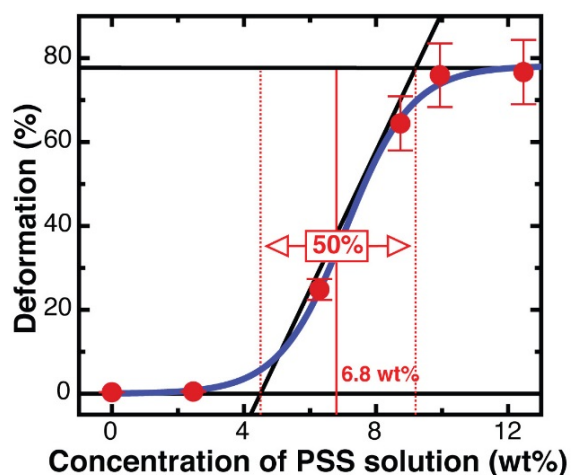


**Fig. 3** Percentage of deformed capsules with six polymer layers as a function of the PSS solution concentration. Each data point is obtained by analysing at least 500 capsules. The red straight lines illustrate how the critical PSS concentration ( $\sim 6.8$  wt%) was obtained.

Polymer Capsule Layer Number	Critical Concentration of PSS solution (wt%)	Critical Osmotic Pressure $P_c$ (kPa)
4	3.1	206
6	6.8	478
8	8.8	643
10	12.3	956

**Table 1** Critical PSS solution concentration and corresponding critical pressure for capsules consisting of four, six, eight, and ten polymer layers.

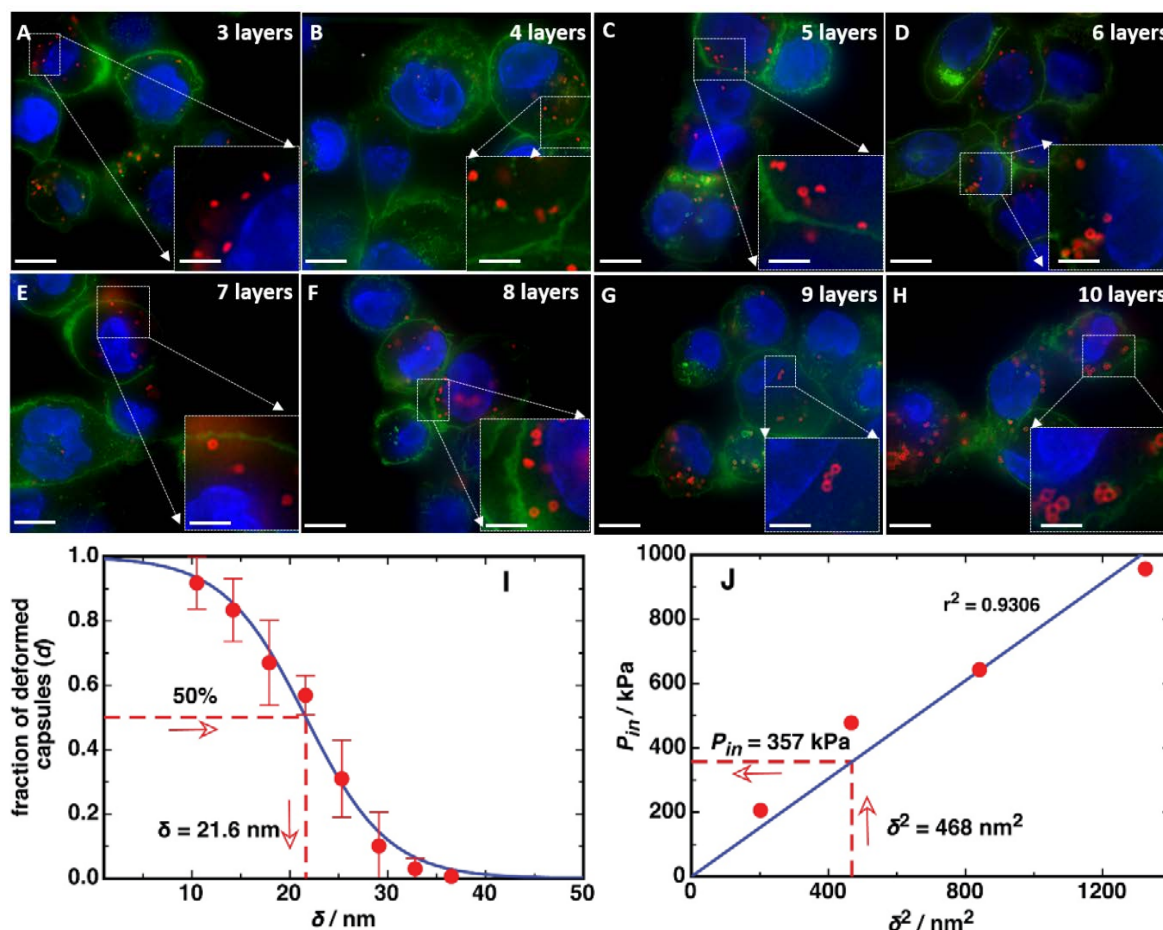


**Fig. 4** SIM images of AF633-labelled PMA capsules (red) with a different number of polymer layers in dTHP-1 cells. Capsules with three to ten layers (A-H, respectively) were incubated with dTHP-1 cells for 12 h at 37 °C, 5% CO<sub>2</sub>. Cell membranes were stained with AF488 WGA (green) and nuclei were stained with Hoechst 33342 (blue). Images represent the maximum intensity projection. Scale bars in A-H are 10 μm. The insets of A-H show higher magnification of the corresponding images and the scale bars are 3.3 μm. (I) The deformation percentage of polymer capsules inside cells (mean ± standard deviation) as a function of capsule film thickness  $\delta$ , which was obtained by counting at least 500 internalised capsules. The solid blue line is the fit of Equation 2. (J) The critical pressure  $P_{in}$  as a function of the square of polymer capsule film thickness  $\delta^2$  (pressure-thickness calibration curve).

The percentage of deformed capsules as a function of the concentration of PSS solution was obtained by counting at least 500 capsules from each PSS solution (Fig. 3). A typical sigmoidal curve of deformation percentage versus PSS concentration with two plateaus was observed, demonstrating that the capsules deform at a critical concentration of PSS. The critical PSS concentration, which is defined as the concentration where the initial spherical capsule shape becomes unstable and then deformed, was analysed through a three tangent evaluation technique, as per Gao et al.'s report (shown as red lines in Fig. 3).<sup>18</sup> Specifically, for the capsules made of six polymer layers, the critical PSS concentration was obtained from the average value of the lower plateau of PSS concentration (~4.5 wt%) and the higher plateau of PSS concentration (~9.2 wt%). Therefore, the critical PSS concentration for the capsules with six polymer layers is ~6.8 wt% and the corresponding calculated critical osmotic pressure is ~478 kPa, based on a calibration curve of osmotic pressure versus PSS concentration (Fig. S4, ESI<sup>†</sup>). The

deformation percentage of capsules with four, six, eight, and ten polymer layers was analysed through the same method (Fig. S5, ESI<sup>†</sup>) and summarised in Table 1.

With an increase in the number of polymer layers, the corresponding critical pressure increases, indicating that the mechanical stability of the polyelectrolyte capsules increases with polymer layers.<sup>10</sup> This is supported by our previous study, showing that the mechanical properties of multilayered films can be controlled by tuning the number of polymer layers.<sup>9</sup> The dependence of the critical osmotic pressure ( $P_c$ ) on the elastic modulus, thickness and radius of the capsules at constant radius, elastic modulus, and negligible plastic deformability, is expected to follow

$$P_c = 4\mu\left(\frac{\delta}{R}\right)^2, \quad (1)$$

where  $\mu$  is the elastic modulus of the capsules,  $\delta$  is the film thickness of the capsule shell, and  $R$  is the radius of the capsule.<sup>18,24</sup> Thus, the critical pressure was plotted against the

square of capsule film thickness (termed as pressure-thickness calibration curve) (Fig. 4J) to confirm the validity of the model and to extrapolate the capsule buckling pressure as a function of thickness.

Next, the intracellular deformation of PMA capsules composed of different polymer layers (three to ten layers) was investigated by incubating dTHP-1 cells with the capsules at a cell-to-capsule ratio of 1:100 for 12 h at 37 °C. Cells were fixed after incubation, and then cell membranes were stained with AF488 wheat germ agglutinin (WGA) and nuclei were stained with Hoechst 33342. The SIM images showed that PMA capsules exhibited different deformation behaviour after internalisation inside dTHP-1 cells depending on the number of polymer layers (Fig. 4A-H). We observed that PMA capsules with three to six layers were mainly compressed and deformed within cells (Fig. 4A-D). In contrast, PMA capsules composed of seven to ten layers largely maintained their original hollow spherical structures inside dTHP-1 cells (Fig. 4E-H). The percentage of deformation as a function of polymer capsule film thickness was obtained by counting at least 500 internalised capsules (Fig. 4I).

To quantify the  $P_{in}$  of dTHP-1 cells, the fraction of deformed capsules as a function of capsule film thickness was plotted (Fig. 4I). The fraction of deformed capsules,  $d$ , was fitted with

$$d(\delta) = \frac{1}{1 + e^{-\alpha(\delta - \beta)}}, \quad (2)$$

where  $\alpha$  is a fitted parameter and  $\beta$  is the value of  $\delta$  that corresponds to  $d=0.5$  (50% deformed), which we find to be  $21.6 \pm 0.4$  nm. From the pressure-thickness calibration curve (Fig. 4J), a pressure of  $\sim 357$  kPa  $\pm 13$  kPa was obtained for a film thickness of  $21.6 \pm 0.4$  nm ( $\delta^2 = 468$  nm<sup>2</sup>). Taken together, our results show that the  $P_{in}$  applied by dTHP-1 cells on the PMA capsules during internalisation is approximately  $\sim 357$  kPa  $\pm 13$  kPa, which corresponds to a maximum intracellular force of  $\sim 0.54$   $\mu$ N on each capsule, given their average diameter of 0.7  $\mu$ m. The PMA capsules do not deform in the presence of serum proteins (see Fig. S2, ESI<sup>†</sup>), nor do they rupture the endosomal/lysosomal membranes (see Fig. S6, ESI<sup>†</sup>), meaning the observed deformation is a consequence of cellular internalisation. Our methods have the assumption that the pressure exerted on the capsules during cellular internalisation may be approximated by the isotropic deformation of capsules ex situ.

This combination of ex situ osmotic pressure-induced deformation experiments and cellular internalisation observations has allowed new information to be gained on the mechanical load on capsules during cellular internalisation. Cell-specific internalisation pressures will be the subject of future investigations.

## Conclusions

In summary, we have applied polymer capsule probes to investigate the mechanical pressure exerted by cells,  $P_{in}$ , during cellular internalisation. By tuning the number of

polymer layers in the capsules, different mechanical properties can be achieved, as confirmed by an osmotic pressure-induced deformation of capsules in PSS solutions. Based on this ex situ pressure study, we investigated the cellular pressure exerted on the polymer capsules during the internalisation process. Our results suggest that human monocyte-derived macrophage dTHP-1 cells exert as high as approximately 357 kPa  $\pm 13$  kPa ( $P_{in}$ ) during internalisation of the polymer capsules. These polymer capsule probes afford a practical approach for the detection of  $P_{in}$  of cells, which is of importance for revealing cell mechanobiology and for designing advanced materials responsive to cellular mechanical forces.

## Acknowledgement

This research was conducted and funded by the Australian Research Council Centre of Excellence in Convergent Bio-Nano Science and Technology (project number CE140100036). This work was also supported by the Australian Research Council (ARC) under the Australian Laureate Fellowship (F. Caruso, FL120100030), Super Science Fellowship (F. Caruso, FS110200025), and Future Fellowship (F. Cavaliere, FT140100873) schemes. We thank Prof. Ray Dagastine (The University of Melbourne), Stuart McDougall (Florey Institute of Neuroscience and Mental Health), and Benjamin Hibbs (Materials Characterisation and Fabrication Platform) for helpful discussions. This work was performed in part at the Materials Characterisation and Fabrication Platform (MCFP) at the University of Melbourne and the Victorian Node of the Australian National Fabrication Facility (ANFF).

## Notes and references

- (1) A. E. Nel, L. Madler, D. Velegol, T. Xia, E. M. Hoek, P. Somasundaran, F. Klaessig, V. Castranova and M. Thompson, *Nat. Mater.*, 2009, **8**, 543-557.
- (2) R. M. Pearson, H.-j. Hsu, J. Bugno and S. Hong, *MRS Bull.*, 2014, **39**, 227.
- (3) L. C. Cheng, X. Jiang, J. Wang, C. Chen and R. S. Liu, *Nanoscale*, 2013, **5**, 3547-3569.
- (4) R. Gomez-Martinez, A. M. Hernandez-Pinto, M. Duch, P. Vazquez, K. Zinoviev, E. J. de la Rosa, J. Esteve, T. Suarez and J. A. Plaza, *Nat. Nanotechnol.*, 2013, **8**, 517-521.
- (5) R. J. Petrie, H. Koo, *Curr. Protoc. Cell Biol.*, 2014, **63**, 12.9.1.
- (6) Y. Yan, G. K. Such, A. P. R. Johnston, H. Lomas and F. Caruso, *ACS Nano*, 2011, **5**, 4252-4257.
- (7) B. Städler, A. D. Price and A. N. Zelikin, *Adv. Funct. Mater.*, 2011, **21**, 14-28.
- (8) J. P. Best, Y. Yan and F. Caruso, *Adv. Healthc. Mater.*, 2012, **1**, 35-47.
- (9) H. Sun, E. H. H. Wong, Y. Yan, J. Cui, Q. Dai, J. Guo, G. G. Qiao and F. Caruso, *Chem. Sci.*, 2015, **6**, 3505-3514.
- (10) R. Palankar, B.-E. Pinchasik, S. Schmidt, B. G. De Geest, A. Fery, H. Möhwald, A. G. Skirtach and M. Delcea, *J. Mater. Chem.*, 2013, **1**, 1175-1181.
- (11) M. F. Bédard, A. Munoz-Javier, R. Mueller, P. del Pino, A. Fery, W. J. Parak, A. G. Skirtach and G. B. Sukhorukov, *Soft Matter*, 2009, **5**, 148-155.
- (12) M. Delcea, S. Schmidt, R. Palankar, P. A. L. Fernandes, A. Fery, H. Möhwald and A. G. Skirtach, *Small*, 2010, **6**, 2858-2862.

- (13) X. Chen, J. Cui, H. Sun, M. Müllner, Y. Yan, K. Noi, Y. Ping and F. Caruso, *Nanoscale*, 2016, **8**, 11924-11931.
- (14) M. P. Neubauer, M. Poehlmann and A. Fery, *Adv. Colloid Interface Sci.*, 2014, **207**, 65-80.
- (15) A. Muñoz Javier, O. Kreft, M. Semmling, S. Kempter, A. G. Skirtach, O. T. Bruns, P. del Pino, M. F. Bedard, J. Rädler, J. Käs, C. Plank, G. B. Sukhorukov and W. J. Parak, *Adv. Mater.*, 2008, **20**, 4281-4287.
- (16) K. Liang, S. T. Gunawan, J. J. Richardson, G. K. Such, J. Cui and F. Caruso, *Adv. Healthc. Mater.*, 2014, **3**, 1551-1554.
- (17) Y. Liu, Y. Tian, Y. Tian, Y. Wang and W. Yang, *Adv. Mater.*, 2015, **27**, 7156-7160.
- (18) C. Gao, E. Donath, S. Moya, V. Dudnik and H. Möhwald, *Eur. Phys. J. E*, 2001, **5**, 21-27.
- (19) A. Fery and R. Weinkamer, *Polymer*, 2007, **48**, 7221-7235.
- (20) A. Fery, F. Dubreuil and H. Möhwald, *New J. Phys.*, 2004, **6**, 18.
- (21) G. B. Sukhorukov, A. Fery, M. Brumen and H. Möhwald, *Phys. Chem. Chem. Phys.*, 2004, **6**, 4078-4089.
- (22) O. Kulygin, A. D. Price, S. F. Chong, B. Städler, A. N. Zelikin and F. Caruso, *Small*, 2010, **6**, 1558-1564.
- (23) S.-F. Chong, J. H. Lee and A. N. Zelikin, F. Caruso, *Langmuir*, 2011, **27**, 1724-1730.
- (24) A. V. Pogorelov, *Bendings of Surfaces and Stability of Shells*, American Mathematical Society, USA 1988.